

# Synthesis and Structural Comparison of $\text{Tp}^{\text{iPr}_2}\text{Rh}[\text{cis-1,2-bis(diphenylphosphino)ethene}]$ : Factors Determining Hapticity ( $\kappa^2$ vs $\kappa^3$ ) of the $\text{Tp}^{\text{iPr}_2}$ Ligand in $\text{Tp}^{\text{iPr}_2}\text{Rh}(\text{diphosphine})$ Complexes

Munetaka Akita,\* Mariko Hashimoto, Shiro Hikichi, and Yoshihiko Moro-oka

Chemical Resources Laboratory, Tokyo Institute of Technology, 4259 Nagatsuta, Midori-ku, Yokohama 226-8503, Japan

Received April 27, 2000

**Summary:** Comparison of structural and spectroscopic features of the  $\text{Rh(I)}$ –diphosphine complexes  $\text{Tp}^{\text{iPr}_2}\text{Rh}(\text{Ph}_2\text{P}-X-\text{PPh}_2)$  reveals that the dominant factor governing hapticity of the  $\text{Tp}^{\text{iPr}_2}$  ligand ( $\kappa^2$  vs  $\kappa^3$ ) is conformation of the central rhodadiphosphacycle. A folded  $\text{RhP}_2\text{X}$  conformation hinders coordination of the pendant pyrazolyl group due to steric repulsion with the bridging part (X) in diphosphine to lead to a  $\kappa^2$ - $\text{Tp}^{\text{iPr}_2}$  species, whereas  $\kappa^3$ -coordination is found in complexes with a flat  $\text{RhP}_2\text{X}$  conformation.

It has been well-documented that (i)  $\text{Tp}^{\text{R}_x}\text{M}(\text{L}_2)$ -type  $\text{d}^8$  metal complexes adopt a four-coordinate square-planar geometry with the  $\kappa^2$ - $\text{Tp}^{\text{R}_x}$  ligand and a five-coordinate square-pyramidal (or trigonal-bipyramidal) geometry with the  $\kappa^3$ - $\text{Tp}^{\text{R}_x}$  ligand and (ii) these geometries can be interconverted with each other via coordination–dissociation–pseudorotation processes of the  $\text{Tp}^{\text{R}_x}$  moiety, as shown in Scheme 1.<sup>1,2</sup> When pseudorotation of the  $\text{Tp}^{\text{R}_x}$  ligand associated with the hapticity change occurs at a rate faster than the  $^1\text{H}$  NMR time scale, all three  $\text{pz}^{\text{R}_x}$  rings<sup>2</sup> are averaged and it is not always facile to determine the hapticity of the  $\text{Tp}^{\text{R}_x}$  ligand by spectroscopic methods alone.<sup>3</sup> In our laboratory,<sup>4</sup>  $\text{Tp}^{\text{iPr}_2}\text{Rh}(\text{L}_2)$ -type complexes were synthesized as precursors for peroxo complexes,<sup>4c</sup> and in a previous paper,<sup>4b</sup> we reported the synthesis and structures of a series of  $\text{Tp}^{\text{iPr}_2}\text{Rh}[\text{Ph}_2\text{P}-(\text{CH}_2)_n-\text{PPh}_2]$  complexes with an  $\alpha,\omega$ -bis(diphenylphosphino)alkane chelate ( $n = 1$  (**1**), 2 (**2**), 3 (**3**); Scheme 1). It was also pointed out that the structure and fluxional behavior of the  $\text{Tp}^{\text{iPr}_2}$  ligand depends on the chelate size; i.e., as the chelate size ( $n$ ) increases, the structure switches from an  $\text{spy}$  ( $\kappa^3$ ) structure to an  $\text{spl}$  ( $\kappa^2$ ) structure<sup>2</sup> and the pseudorotation becomes slower. The monotonically changing  $\text{P}-\text{Rh}-\text{P}$  bite angles (see Table 2) were considered as indicators of the steric congestion brought about by the  $\text{PPh}_2$  groups. However, addition of the data for the *cis*-1,2-bis(diphenylphosphino)ethene (dppene) complex **4** described herein caused failure in the monotonic relationship. Although the  $\text{dppe}$  (**2**) and  $\text{dppene}$  complexes (**4**)

contain diphosphine ligands with a  $\text{C}_2\text{H}_x$  bridge, their properties are considerably different. Despite so many studies, including our work, no conclusive interpretation of these structural aspects has been presented so far.<sup>1,3</sup> This note describes the synthesis and characterization of  $\text{Tp}^{\text{iPr}_2}\text{Rh}(\text{dppene})$  (**4**),<sup>2</sup> and structural comparison with **1–3** reveals that the dominant factor determining the hapticity and dynamic behavior of the  $\text{Tp}^{\text{iPr}_2}$  ligand is

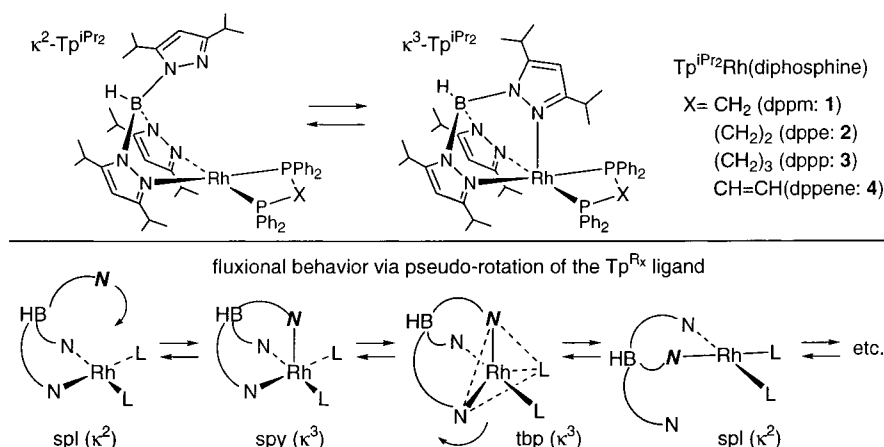
(3)  $\text{Tp}^{\text{R}_x}\text{Rh}$  complexes have been studied most extensively. Diene complexes: (a) Cocivera, M.; Desmond, T. J.; Ferguson, G.; Kaitner, B.; Lalor, F. J.; O'Sullivan, D. J. *Organometallics* **1982**, *1*, 1125. (b) Cocivera, M.; Ferguson, G.; Kaitner, B.; Lalor, F. J.; O'Sullivan, D. J.; Parvez, M.; Ruhl, B. *Organometallics* **1982**, *1*, 1132. (c) Cocivera, M.; Ferguson, G.; Lalor, F. J.; Szczecinski, P. *Organometallics* **1982**, *1*, 1139. (d) Bucher, U. E.; Currao, A.; Nesper, R.; Rüegger, H.; Venanzi, L. M.; Younger, E. *Inorg. Chem.* **1995**, *34*, 66. (e) Bucher, U. E.; Fässler, T. F.; Hunziker, M.; Nesper, R.; Rüegger, H.; Venanzi, L. M. *Gazz. Chim. Ital.* **1995**, *125*, 181. (f) Sanz, D.; Santa Maria, M. D.; Claramunt, R. M.; Cano, M.; Heras, J. V.; Campo, J. A.; Ruiz, F. A.; Pinilla, E.; Monge, A. *J. Organomet. Chem.* **1996**, *526*, 341. CO and isonitrile complexes: (g) Trofimenko, S. *Inorg. Chem.* **1971**, *10*, 1372. (h) Ghosh, C. K.; Graham, W. A. G. *J. Am. Chem. Soc.* **1987**, *109*, 4726. (i) Ghosh, C. K.; Graham, W. A. G. *J. Am. Chem. Soc.* **1989**, *111*, 375. (j) Jones, W. D.; Hessel, E. T. *Inorg. Chem.* **1991**, *30*, 778. (k) Hessel, E. T.; Jones, W. D. *Organometallics* **1992**, *11*, 1496. (l) Jones, W. D.; Hessel, E. T. *J. Am. Chem. Soc.* **1992**, *114*, 6087. (m) Jones, W. D.; Hessel, E. T. *J. Am. Chem. Soc.* **1993**, *115*, 554. (n) Rheingold, A. L.; Ostrander, R. L.; Haggerty, B. S.; Trofimenko, S. *Inorg. Chem.* **1993**, *33*, 3666. (o) Keyes, M. C.; Young, V. G., Jr.; Tolman, W. B. *Organometallics* **1996**, *15*, 4133. (p) Chauby, V.; Le Berre, S.; Daran, J.-C.; Commenges, G. *Inorg. Chem.* **1996**, *35*, 6345. (q) Connelly, N. G.; Emslie, D. J. H.; Metz, B.; Orpen, A. G.; Quayle, M. J. *J. Chem. Soc., Chem. Commun.* **1996**, 2289. (r) Purwoko, A. A.; Lees, A. J. *Inorg. Chem.* **1996**, *35*, 675. (s) Dhosh, C. K.; Rodgers, D. P. S.; Graham, W. A. G. *J. Chem. Soc., Chem. Commun.* **1988**, 1511. (t) Northcutt, T. O.; Lachicotte, R. J.; Jones, W. D. *Organometallics* **1998**, *17*, 5148. (u) Wick, D. D.; Northcutt, T. O.; Lachicotte, R. J.; Jones, W. D. *Organometallics* **1998**, *17*, 4484. Olefin complexes: (v) Trofimenko, S. *J. Am. Chem. Soc.* **1969**, *91*, 588. (w) Oldham, W. J.; Heinekey, D. M. *Organometallics* **1997**, *16*, 467. (x) Pérez, P. J.; Poveda, M. L.; Carmona, E. *Angew. Chem., Int. Ed. Engl.* **1995**, *34*, 66. (y) Alvalado, Y.; Boutry, O.; Gutiérrez, E.; Monge, A.; Nicasio, M. C.; Pérez, P. J.; Poveda, M. L.; Ruiz, C.; Bianchini, C.; Carmona, E. *Chem. Eur. J.* **1997**, *3*, 860. (z) Gutiérrez-Puebla, E.; Monge, A.; Nicasio, M. C.; Pérez, P. J.; Poveda, M. L.; Rey, L.; Ruiz, C.; Carmona, E. *Inorg. Chem.* **1998**, *37*, 4538. (aa) Nicasio, M. C.; Paneque, M.; Pérez, P. J.; Pizzano, A.; Poveda, M. L.; Rey, L.; Sirol, S.; Taboada, S.; Trujillo, M.; Monge, A.; Ruiz, C.; Carmona, E. *Inorg. Chem.* **2000**, *39*, 180. Phosphine complexes: Hill, A. F.; White, A. J. P.; Williams, D. J.; Wilton-Ely, J. D. E. *Organometallics* **1998**, *17*, 3152. Rh(III) and polyhydride complexes: (bb) May, S.; Reialu, P.; Powell, J. *Inorg. Chem.* **1980**, *19*, 1582. (cc) Bucher, U. E.; Lengweiler, D.; von Philipsborn, W.; Venanzi, L. M. *Angew. Chem., Int. Ed. Engl.* **1990**, *29*, 548. (dd) Eckert, J.; Albinati, A.; Bucher, U. E.; Venanzi, L. M. *Inorg. Chem.* **1996**, *35*, 1292. (ee) See also our papers cited in ref 4.

(4) Our recent works based on  $\text{Tp}^{\text{R}_x}\text{Rh}$  systems: (a) Akita, M.; Ohta, K.; Takahashi, Y.; Hikichi, S.; Moro-oka, Y. *Organometallics* **1997**, *16*, 4121. (b) Ohta, K.; Hashimoto, M.; Takahashi, Y.; Hikichi, S.; Akita, M.; Moro-oka, Y. *Organometallics* **1999**, *18*, 3234. (c) Takahashi, Y.; Hashimoto, M.; Hikichi, S.; Akita, M.; Moro-oka, Y. *Angew. Chem., Int. Ed.* **1999**, *38*, 3074.

(1) (a) Trofimenko, S. *Chem. Rev.* **1993**, *93*, 943. (b) Trofimenko, S. *Scorpionates: The Coordination Chemistry of Polypyrazolylborate Ligands*; Imperial College Press: London, England, 1999. (c) Kitajima, N.; Tolman, W. B. *Prog. Inorg. Chem.* **1995**, *43*, 419.

(2) Abbreviations used in this paper:  $\text{Tp}^{\text{R}_x}$  = substituted Tp derivatives;  $\text{Tp}^{\text{iPr}_2}$  = hydridotris(3,5-diisopropylpyrazolyl)borate;<sup>1a,b</sup>  $\text{pz}^{\text{R}_x}$  = substituted pyrazolyl ring;  $\text{pz}^{\text{iPr}_2}$  = 3,5-diisopropylpyrazolyl ring; 4- $\text{pz}^{\text{iPr}_2}$ -H = the 4-pyrazolyl proton in  $\text{pz}^{\text{iPr}_2}$ ;  $\text{coe}$  = cyclooctene;  $\text{spl}$  = square planar;  $\text{spy}$  = square pyramidal;  $\text{tbp}$  = trigonal bipyramidal.

Scheme 1

Table 1. Selected Structural Parameters for 4<sup>a</sup>

Interatomic Distances			
Rh1–P1	2.205(2)	Rh1–N31	2.893(4)
Rh1–P2	2.216(1)	P1–C1	1.818(6)
Rh1–N11	2.130(6)	P2–C2	1.821(9)
Rh1–N21	2.103(4)		
Bond Angles			
P1–Rh1–P2	84.57(6)	P2–Rh1–N11	97.9(1)
P1–Rh1–N11	174.7(1)	P2–Rh1–N21	177.5(2)
P1–Rh1–N21	97.8(2)	N11–Rh1–N21	79.7(2)

<sup>a</sup> Interatomic distances in Å and bond angles in deg.

steric repulsion between the pendant  $\text{pz}^{\text{iPr}_2}$  ring and the bridging part of the diphosphine ligand.

The dppene complex **4** was synthesized by following the method developed in our laboratory: i.e., treatment of the labile precursor,  $\text{Tp}^{\text{iPr}_2}\text{Rh}(\text{coe})(\text{MeCN})$ ,<sup>2</sup> with dppene.<sup>4b</sup> The  $\nu_{\text{BH}}$  value ( $2534 \text{ cm}^{-1}$ ) indicates  $\kappa^3$ -coordination of the  $\text{Tp}^{\text{iPr}_2}$  ligand,<sup>5</sup> and a single 4- $\text{pz}^{\text{iPr}_2}$ -H singlet signal ( $^1\text{H}$  NMR)<sup>2</sup> indicated occurrence of a dynamic process, which was frozen below  $-35^\circ\text{C}$  to give a 1H:2H mirror-symmetrical pattern. The molecular structure of **4** was determined by X-ray crystallography,<sup>6</sup> and an ORTEP view and selected structural parameters are shown in Figure 1 and Table 1, respectively. The square-planar coordination geometry of the basal  $\text{RhP}_2\text{N}_2$  moiety in **4** is very similar to those of the previously reported diphosphine complexes **1–3**.<sup>4b</sup> It is notable that the  $\text{Rh1}\cdots\text{N31}$  distance (2.893(4) Å) is substantially longer than the other two Rh–N distances in the coordination plane ( $\sim 2.1$  Å) but is still smaller than the sum of van der Waals radii (3.4 Å). In addition, the arrangement of the pendant  $\text{pz}^{\text{iPr}_2}$  ring with the lone pair electrons of the N31 atom projecting toward the rhodium center indicates the presence of an attractive interaction between N31 and Rh1, in accord with the  $\nu_{\text{BH}}$  value, suggesting  $\kappa^3$ -coordination. Thus, the dppene complex **4** is characterized as a five-coordinate square-pyramidal species with the  $\kappa^3$ - $\text{Tp}^{\text{iPr}_2}$  ligand (spy ( $\kappa^3$ )).

In Table 2, selected spectroscopic and structural features of the dppene complex **4** are compared with those of the related diphosphine complexes **1–3** and the dicarbonyl complex  $\text{Tp}^{\text{iPr}_2}\text{Rh}(\text{CO})_2$  (**5**).<sup>4b</sup> The complexes are arranged by taking into account the  $\text{Rh1}\cdots\text{N31}$  distances and the  $^1\text{H}$  NMR and IR features. The dppp

complex (**3**) exists as an spl ( $\kappa^2$ ) species in both the solid and solution states, and pseudorotation via the  $\kappa^2$ – $\kappa^3$  interconversion is much slower than the  $^1\text{H}$  NMR coalescence time scale at room temperature. The situation of the dpe complex **2** is similar to **3**, but the pseudorotation rate is comparable to the NMR time scale. The coordination geometry of the dppene **4** and dicarbonyl complexes **5** is spy ( $\kappa^3$ ), and the three 4- $\text{pz}^{\text{iPr}_2}$ -H signals are observed as single sharp singlets, indicating very fast pseudorotation. The dppm complex **1** is between (see below). As mentioned in the introductory part, addition of **4** caused failure in the monotonic relationship between the structural change and the P–Rh–P bite angle. Therefore, we sought other criteria to interpret these results.

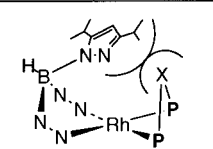
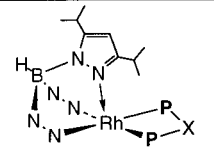
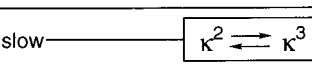
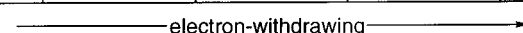
Let us point out that remarkable differences are noted for the conformation of the rhodadiphosphacycle ( $\text{RhPXP}$ ) and the arrangement of the phenyl groups attached to the coordinated phosphorus atoms. As typical examples, structures of the core parts of **2** and **4** are compared in Figure 2.

In the case of the dpe (**2**) and dppp complexes (**3**) containing the flexible  $(\text{CH}_2)_n$ -alkylene linkers (X), the diphosphine bridges (X) are folded up from the square-planar  $\text{RhN}_2\text{P}_2$  coordination plane. The rhodadiphosphacyclopentane moiety in the dpe complex **2** (Figure 2a) adopts an envelope conformation, which also causes the widely spread arrangement of the two phenyl rings. Steric repulsion between the out-of-plane  $\text{CH}_2\text{CH}_2$  bridge and the pendant  $\text{pz}^{\text{iPr}_2}$  ring is relieved by rotation of the  $\text{pz}^{\text{iPr}_2}$  ring around the B1–N32 bond to result in the  $\kappa^2$ -coordination of the  $\text{Tp}^{\text{iPr}_2}$  ligand. The  $\text{pz}^{\text{iPr}_2}$  ring is laid over the Rh center to be accommodated in the space above the spread phenyl groups (see the space-filling model in Figure 2a). The extent of the folding of the chelate rings can be evaluated by the dihedral angles ( $\theta_1$ ) between the  $\text{RhN}_2\text{P}_2$  and P–C $\cdots$ C–P least squares planes. The  $\theta_1$  values for **2** and **3** ( $>40^\circ$ ) are substantially larger than those for the dppene (**4**:  $6.9^\circ$ ) and dppm complexes (**1**:  $11.8^\circ$ ), which contain a flat and rigid  $\text{RhPXP}$  chelate ring. As shown in Figure 2b, the

(5) The hapticity of  $\text{Tp}^{\text{R}_x}$  ligands can be determined by their  $\nu(\text{B–H})$  ( $\kappa^2 < 2500 \text{ cm}^{-1} < \kappa^3$ )<sup>4a</sup> or  $\delta_{\text{B}}$  values ( $\kappa^3 < -8 \text{ ppm} < \kappa^2$ ).<sup>3t</sup>

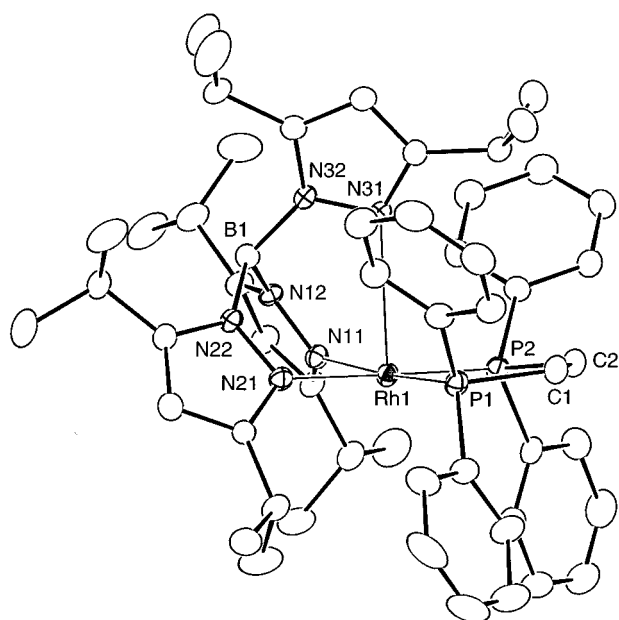
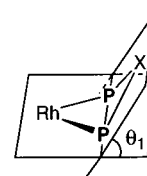
(6) Details of X-ray crystallography are described in the Supporting Information. Crystal data for **4**· $\text{CH}_2\text{Cl}_2$ : formula  $\text{C}_{54}\text{H}_{70}\text{BN}_6\text{P}_2\text{Cl}_2\text{Rh}$ , formula weight 1048.72, monoclinic, space group  $C2/c$ ,  $a = 40.548(6)$  Å,  $b = 14.205(4)$  Å,  $c = 24.967(11)$  Å,  $\beta = 127.675(15)^\circ$ ,  $V = 11382(6)$  Å<sup>3</sup>,  $Z = 8$ ,  $d_{\text{calc}} = 1.23 \text{ g cm}^{-3}$ ,  $\mu = 0.489 \text{ cm}^{-1}$ ,  $R1 = 0.072$  for the 8382 unique data with  $F > 4\sigma(F)$  ( $wR2 = 0.200$  for all 9819 data) and 607 parameters.

**Table 2.** Comparison of Structural and Spectroscopic Features of  $\text{Tp}^{\text{iPr}_2}\text{Rh}(\text{L}_2)$  Complexes

ligand	dppp (3)	dppe (2)	dppm (1)	dppene (4)	(CO) <sub>2</sub> (5)
X-ray crystallography	 $\kappa^2$		 $\kappa^3$		
Rh1...N31 <sup>a</sup>	3.381(5)	3.419(7)	3.081(3)	2.893(4)	2.33(1)
$\theta_1$ <sup>b,c</sup>	43.8	45.8	11.8	6.9	2.8
$\theta_2$ <sup>c,d</sup>	56.7(5)	57.6(6)	44.4(2)	17.4(5)	2(1)
<P-Rh-P <sup>c</sup>	88.17(5)	80.90(6)	73.12(4)	84.57(6)	83(1)
<sup>1</sup> H-NMR	pseudo-rotation of the $\text{Tp}^{\text{iPr}_2}$ ligand via $\kappa^2$ - $\kappa^3$ interconversion				
	$\kappa^2$				
4- $\text{pz}^{\text{iPr}_2}$ -H signals at r.t. [coalescence temperature]	1H : 2H (sharp) [> r.t.]	3H <sup>e</sup> (broad) [0°C]	3H <sup>e</sup> (sharp) [-95°C]	3H <sup>e</sup> (sharp) [-35°C]	3H <sup>e</sup> (sharp) [<-95°C]
IR	$\kappa^2$		$\kappa^3$		
$\nu_{\text{BH}}$ <sup>f</sup>	2488	2486	2488	2534	2547
$E_{\text{L}}$ <sup>g</sup>	0.42	0.36	0.43	0.49	0.99
					

<sup>a</sup> in Å. <sup>b</sup> dihedral angles between  $\text{RhN}_2\text{P}_2$  and C-P...P-C mean planes. <sup>c</sup> in deg. <sup>d</sup> Rh1...B1-N32-N31 dihedral angles. <sup>e</sup> coalesced signals. <sup>f</sup> observed as KBr pellets (in  $\text{cm}^{-1}$ ).

<sup>g</sup> See ref. 7.

**Figure 1.** Molecular structure of **4** drawn at the 30% probability level.

flat and rigid rhodadiphosphacyclopentene in **4** is virtually coplanar with respect to the  $\text{RhP}_2\text{N}_2$  coordination plane, and the situation of the dppm complex (**1**) is essentially the same as that of **4**. The coplanar arrangement causes no severe steric hindrance between the pendant  $\text{pz}^{\text{iPr}_2}$  ring and X to lead to  $\kappa^3$ -coordination

of the  $\text{Tp}^{\text{iPr}_2}$  ligand. As a result of the planar conformation, the phenyl rings are projected above and below the chelate plane to form a wedge-shaped pocket above the rhodium atom, and the pendant  $\text{pz}^{\text{iPr}_2}$  ring fits into the pocket to be coordinated to the metal center. Let us add some comments on the dppm complex (**1**). The  $\nu_{\text{BH}}$  value suggests  $\kappa^2$ -coordination, but the  $\text{Rh}\cdots\text{N}$  distance falls on the borderline between  $\kappa^2$ - and  $\kappa^3$ -coordination. It is also notable that the projection of lone pair electrons of the nitrogen atom in the pendant  $\text{pz}^{\text{iPr}_2}$  group (corresponding to N31 in **4**) is slightly deviated from the metal center, and the deviation can be estimated from the  $\text{Rh1}\cdots\text{B1}-\text{N32}-\text{N31}$  dihedral angles ( $\theta_2 = 0$  for an ideal  $\kappa^3$ -form) shown in Table 2. Judging from the  $\text{Rh1}\cdots\text{N31}$  distance and the  $\theta_2$  value for **1** located between the two extremes,  $\kappa^2$  (**2**, **3**) and  $\kappa^3$  (**4**, **5**), coordination of the pendant  $\text{pz}^{\text{iPr}_2}$  group in **1** may be rather weak, but significant steric repulsion to prevent a more strongly bound  $\kappa^3$ -coordination is *not* present in a manner similar to **4**.

The electronic effect of the diphosphine ligands operates synergistically. A  $\kappa^3$ - $\text{Tp}^{\text{iPr}_2}$  form should be favored, as the metal center becomes more Lewis acidic. According to the  $E_{\text{L}}$  value defined by Lever,<sup>7</sup> dppene is more electron-withdrawing than phosphine derivatives and, therefore, the metal center becomes more electron-deficient to induce coordination of the third pyrazolyl group: i.e.,  $\kappa^3$ -coordination.

(7) Lever, A. B. P. *Inorg. Chem.* **1990**, 29, 1271.



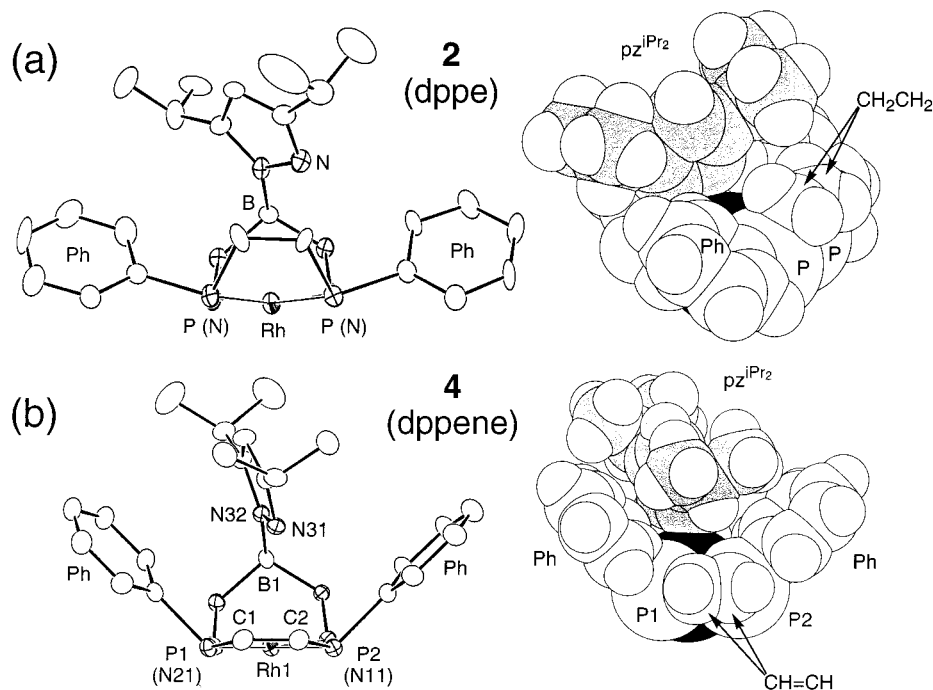


**Figure 2.** Side views and space-filling models of the core parts of **2** (a) and **4** (b). Non-hydrogen atoms of the pendant  $\text{pz}^{\text{iPr}_2}$  groups are shaded.

The dicarbonyl complex **5**<sup>4b</sup> is an extreme case in the present series of compounds, because the  $(\text{CO})_2$  system does not contain a chelating moiety as the diphosphine ligands have and is much more electron-withdrawing than phosphines. Thus,  $\kappa^3$ -coordination features of the  $\text{Tp}^{\text{iPr}_2}$  ligand are obvious for **5**, in accord with the above discussion.<sup>8</sup>

Through the present study, the virtually parallel relationship among  $\text{Rh1}\cdots\text{N31}$  distance, hapticity,  $\theta_1$  and  $\theta_2$  values, and coalescence temperature of the  $4\text{-pz}^{\text{iPr}_2}\text{-H}$  signals has been established for the series of  $\text{Tp}^{\text{iPr}_2}\text{Rh}(\text{diphosphine})$  complexes. In other words, (1) the hapticity of the  $\text{Tp}^{\text{iPr}_2}$  ligand ( $\kappa^2$  vs  $\kappa^3$ : characterized by  $\text{Rh1}\cdots\text{N31}$  distance and  $\theta_2$ ) is governed by the conformation of the  $\text{RhP}_2\text{X}$  moiety (folded or flat: characterized by  $\theta_1$ ) and (2) the rate of pseudorotation of the  $\text{Tp}^{\text{iPr}_2}$  ligand (characterized by coalescence temperature) involving the  $\kappa^2$ – $\kappa^3$  interconversion is strongly dependent on the ease of formation of a  $\kappa^3$  species.<sup>9</sup> A folded  $\text{RhP}_2\text{X}$  chelate (with large  $\theta_1$ ) hinders coordination of the pendant  $\text{pz}^{\text{iPr}_2}$  group due to steric repulsion with the  $\text{X}$  moiety to result in a  $\kappa^2$ -coordination, whereas a flat and rigid  $\text{RhP}_2\text{X}$  chelate leads to a  $\kappa^3$ -species.

## Experimental Section

**General Methods.** All manipulations were carried out under an Ar atmosphere using standard Schlenk tube techniques.  $\text{CH}_2\text{Cl}_2$  ( $\text{P}_4\text{O}_{10}$ ), hexane (Na–K alloy), and MeCN ( $\text{CaH}_2$ ) were treated with appropriate drying agents, distilled, and stored under argon.  $^1\text{H}$  NMR spectra were recorded on

Bruker AC200 (200 MHz) and JEOL EX-400 spectrometers (400 MHz; low-temperature measurements). Benzene- $d_6$  for NMR measurements containing 0.5% TMS was dried over molecular sieves, degassed, distilled under reduced pressure, and stored under Ar. IR spectra were obtained on a JASCO FT/IR 5300 spectrometer.  $\text{Tp}^{\text{iPr}_2}\text{Rh}(\text{coe})(\text{MeCN})\cdot n\text{MeCN}$  compounds were prepared according to the reported method, and the  $n$  value was determined by a  $^1\text{H}$  NMR measurement of each sample.<sup>4c</sup>  $\text{dppene}$  was purchased and used as received.

**Preparation of 4.** To a  $\text{CH}_2\text{Cl}_2$  solution (4 mL) of  $\text{Tp}^{\text{iPr}_2}\text{Rh}(\text{coe})(\text{MeCN})\cdot 15\text{MeCN}$  (470 mg, 0.352 mmol) was added  $\text{dppene}$  (140.7 mg, 0.355 mmol), and the mixture was stirred for 1.5 h at ambient temperature. After removal of the volatiles under reduced pressure the residue was washed with MeCN and then dried under reduced pressure. Recrystallization of the residue from  $\text{CH}_2\text{Cl}_2$ –hexane gave **4** as dark brown prisms (217 mg, 0.225 mmol, 64% yield). **4**:  $^1\text{H}$  NMR ( $\text{C}_6\text{D}_6$ )  $\delta_{\text{H}}$  7.65–7.05 (22H, m, Ph and HC=), 5.84 (3H, s,  $4\text{-pz}^{\text{iPr}_2}\text{H}$ ), 3.69 (3H, sept,  $J = 6.8$  Hz,  $\text{CH}(\text{CH}_3)_2$ ), 3.09 (3H, m,  $\text{CH}(\text{CH}_3)_2$ ), 1.24 (18H, d,  $J = 6.8$  Hz,  $\text{CH}(\text{CH}_3)_2$ ), 1.07 (18H, br,  $\text{CH}(\text{CH}_3)_2$ ); IR (KBr)  $\nu_{\text{BH}}$  2534  $\text{cm}^{-1}$ . Anal. Calcd for  $\text{C}_{53.5}\text{H}_{69}\text{BN}_6\text{P}_2\text{ClRh}$  ( $4\cdot 0.5\text{CH}_2\text{Cl}_2$ ): C, 63.79; H, 6.90; N, 8.34. Found: C, 64.10; H, 6.99; N, 8.39.

**Acknowledgment.** We are grateful to the Ministry of Education, Science, Sports and Culture of the Japanese Government for financial support of this research (Grants-in-Aid for Scientific Research: 08102006 and 11228201).

**Supporting Information Available:** Experimental details for X-ray crystallography and crystallographic results. This material is available free of charge via the Internet at <http://pubs.acs.org>.

OM0003640

(8) The steric considerations may be able to be extended to diene complexes.<sup>4a</sup> As we reported previously, for  $\text{Tp}^{\text{iPr}_2}\text{Rh}(1,5\text{-cyclooctadiene})$  the  $\kappa^2$  structure is detected as the sole species by IR, whereas  $\text{Tp}^{\text{iPr}_2}\text{-Rh}(\text{norbornadiene})$  contains almost equal amounts of  $\kappa^2$  and  $\kappa^3$  (tbp) species. The  $\text{CH}_2\text{CH}_2$  moiety in cod should cause steric repulsion with the pendant pyrazolyl ring to prevent formation of a  $\kappa^3$  species, and in the case of nbd, the alkylene moiety is tied by the methylene bridge to reduce the steric interaction with the pendant pyrazolyl ring.

(9) The coalescence temperature of the  $\text{dppene}$  complex **4** is not so low, as expected from the series. The discontinuity may be a result of kinetic problems of other stages of the dynamic process, because the pseudorotation involves not only the  $\kappa^2$ – $\kappa^3$  hapticity change but also such processes as  $\text{spy}$ – $\text{tbp}$  isomerization as shown in Scheme 1.